

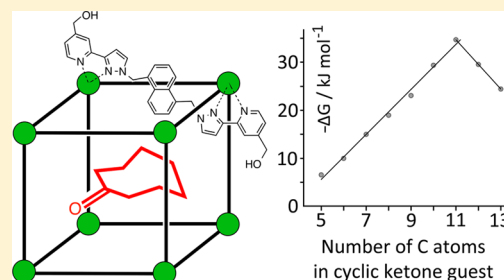
# Mapping the Internal Recognition Surface of an Octanuclear Coordination Cage Using Guest Libraries

Simon Turega, William Cullen, Martina Whitehead, Christopher A. Hunter,\* and Michael D. Ward\*

Department of Chemistry, University of Sheffield, Sheffield S3 7HF, U.K.

**S** Supporting Information

**ABSTRACT:** Size and shape criteria for guest binding inside the cavity of an octanuclear cubic coordination cage in water have been established using a new fluorescence displacement assay to quantify guest binding. For aliphatic cyclic ketones of increasing size (from C<sub>5</sub> to C<sub>11</sub>), there is a linear relationship between  $\Delta G$  for guest binding and the guest's surface area: the change in  $\Delta G$  for binding is 0.3 kJ mol<sup>-1</sup> Å<sup>-2</sup>, corresponding to 5 kJ mol<sup>-1</sup> for each additional CH<sub>2</sub> group in the guest, in good agreement with expectations based on hydrophobic desolvation. The highest association constant is  $K = 1.2 \times 10^6$  M<sup>-1</sup> for cycloundecanone, whose volume is approximately 50% of the cavity volume; for larger C<sub>12</sub> and C<sub>13</sub> cyclic ketones, the association constant progressively decreases as the guests become too large. For a series of C<sub>10</sub> aliphatic ketones differing in shape but not size,  $\Delta G$  for guest binding showed no correlation with surface area. These guests are close to the volume limit of the cavity (cf. Rebek's 55% rule), so the association constant is sensitive to shape complementarity, with small changes in guest structure resulting in large changes in binding affinity. The most flexible members of this series (linear aliphatic ketones) did not bind, whereas the more preorganized cyclic ketones all have association constants of 10<sup>4</sup>–10<sup>5</sup> M<sup>-1</sup>. A crystal structure of the cage-cycloundecanone complex shows that the guest carbonyl oxygen is directed into a binding pocket defined by a convergent set of CH groups, which act as weak hydrogen-bond donors, and also shows close contacts between the exterior surface of the disc-shaped guest and the interior surface of the pseudospherical cage cavity despite the slight mismatch in shape.



## INTRODUCTION

Self-assembled cages and capsules remain of intense interest because they provide straightforward synthetic access to complicated supramolecular assemblies with robust, well-defined three-dimensional structures.<sup>1–5</sup> In the field of coordination cages, appropriate combinations of metal ions and bridging ligands can result in large pseudospherical arrays of remarkable complexity, generally having structures based on high-symmetry polyhedral cores,<sup>1</sup> with large central cavities capable of binding neutral or ionic guests.<sup>3,4</sup> Similarly, purely organic cages relying on covalent bonding or hydrogen bonding between components likewise have a well-developed host–guest chemistry associated with the confined space of the central cavity.<sup>2,5</sup> The host–guest chemistry of such cages and capsules can be exploited in many ways, varying from fundamental studies of molecular recognition properties in confined environments to some remarkable examples of catalysis.<sup>4</sup>

In this contribution, we analyze quantitatively the binding of neutral organic guests in the cavity of a water-soluble coordination cage. The number of studies that have looked in systematic detail at guest binding in coordination cages—to determine shape and size limitations and analyze factors that govern binding affinity—are relatively sparse; in general it has been deemed sufficient to know that a specific target guest binds well or that a particular reaction is catalyzed. The types of

non-covalent interaction leading to guest binding are of course well-known. Electrostatic interactions are readily identified in some cases as being responsible for guest binding, as shown by interactions of anionic guests with the vacant axial sites of Pd(II) ions in cationic cages.<sup>6</sup> Custelcean et al.<sup>7</sup> have prepared cages with an internally directed set of urea-based units that form strong hydrogen bonds with oxoanion guests, and Crowley's cisplatin-containing cage complex is also based on hydrogen bonding between the host and guest.<sup>3b</sup> In aqueous solution, the hydrophobic effect is a driving force for binding of nonpolar guests,<sup>8</sup> and in some cases aromatic stacking between the host and guest is also present.<sup>9</sup> Nitschke recently used principal component analysis to disentangle the factors that determine the binding affinity of small organic guests in a family of tetrahedral coordination cages.<sup>10</sup> Rebek's work on hydrogen-bonded organic cages highlights the potential that systematic studies of families of host–guest complexes offer for understanding molecular recognition in supramolecular systems, with analysis of the binding of hydrocarbon guests resulting in the principle that, for optimal occupancy of the space in a cavity by guest molecules, the total volume of guests should be 55 ± 9% of the cavity volume (the “55% rule”).<sup>2a,11</sup>

Received: April 29, 2014

Published: May 19, 2014

We recently studied guest binding in an octanuclear  $M_8L_{12}$  host cage with an approximately cubic structure and a central cavity with a volume of  $407 \text{ \AA}^3$  (Figure 1).<sup>12,13</sup> This cage is one

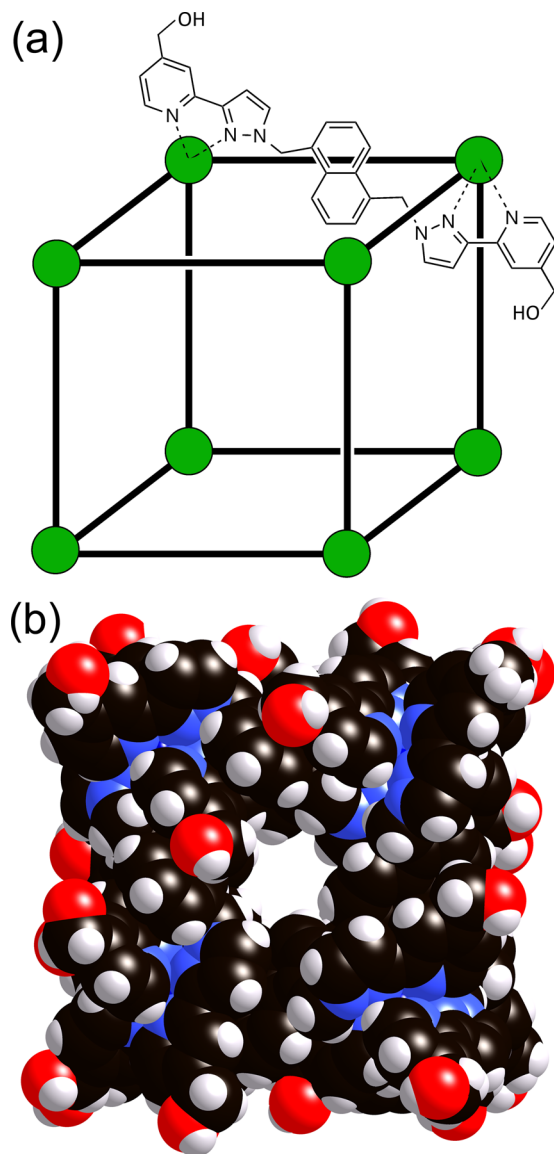


**Figure 1.** Structure of the host cage  $[\text{Co}_8\text{L}_{12}](\text{BF}_4)_{16}$ . (a) Sketch of the octanuclear core showing the disposition of the bridging ligands. (b) Space-filling view of the complete cage cation, showing the external O atoms of the hydroxyl groups in red. Panel (b) is reproduced with permission from ref 13. Copyright 2013 Royal Society of Chemistry.

of an extensive family of coordination cages that we have prepared,<sup>14</sup> and it has proven to be an effective host for organic guests with a coumarin-like bicyclic core as well as monocyclic analogues. We showed that the binding of a series of isostructural bicyclic guests in acetonitrile involved a polar interaction with a convergent set of CH protons on the interior surface of the cage that forms a well-defined binding pocket; there was a clear linear relationship between  $\Delta G^\circ$  for binding and the hydrogen-bond-acceptor parameter ( $\beta$ ) of the guest.<sup>12</sup> In water, however, binding is dominated by the hydrophobic effect, with no contribution to  $\Delta G^\circ$  from polar interactions.<sup>13</sup> The most stable complex in these studies was the 2-

hydroxyquinoline complex (amide tautomer) in water:  $\Delta G^\circ = -22.6 \pm 0.5 \text{ kJ mol}^{-1}$  and  $K = 9100 \pm 2000 \text{ M}^{-1}$ .<sup>13</sup>

Given these promising binding properties, we decided to undertake a more extensive study of binding in the cavity of the cage using a series of related guests that contain the same polar functional group (a ketone) but differ in the size and shape of the alkane framework. Under the assumption that the polar interactions with the ketone group are similar across the series, the differences in binding affinity are related to (i) steric factors based on how well the guest fits in the cavity and (ii) hydrophobic factors based on the total nonpolar surface area of host and guest desolvated on binding.<sup>15</sup>

To make such a survey of multiple guests, automated methods based on optical spectroscopy offer an attractive alternative to NMR spectroscopy for measuring association constants.<sup>16</sup> Accordingly, we developed an automated fluorescence displacement assay<sup>17</sup> for our cage system that allows a large number of guests to be evaluated in parallel. Fluorescence can be used to measure association constants in the range  $10^4$ – $10^9 \text{ M}^{-1}$  and requires very small amounts of host. Having developed and validated the assay, we used it to investigate binding of a series of 19 aliphatic ketones in water, which provided some examples of very strong guest binding and insights into the internal dimensions of the  $M_8L_{12}$  cage.

## RESULTS AND DISCUSSION

**(i). Fluorescence Displacement Assay for Guest Binding.** The host cage used in this work is a  $[\text{Co}_8\text{L}_{12}](\text{BF}_4)_{16}$  cube (Figure 1).<sup>12–14</sup> It was clear from our initial studies that the cavity inside the cubic cage is large enough to bind bicyclic organic guests such as coumarin (and related molecules of similar shape and size).<sup>12,13</sup> In view of the strong fluorescence of some coumarin derivatives, this seemed to be a good place to search for guests that might act as fluorescent reporters of binding inside the cage cavity. The binding of coumarin derivatives is sensitive to the presence of even small substituents at some positions: the cage can tolerate substituents at the C4 position of coumarin that are smaller than an ethoxy group; small substituents (hydroxyl, but not methyl or larger) are tolerated at the C7 position, and C6 must be unsubstituted.<sup>12</sup> After testing various possible guests matching these criteria, we selected 4-methyl-7-aminocoumarin (MAC) as the fluorescent probe: it has an intense fluorescence maximum at 443 nm in water.<sup>18</sup>  $^1\text{H}$  NMR titration with the cage in water showed that MAC binds in slow exchange,<sup>12,13</sup> although MAC is too poorly soluble at NMR concentrations to allow a reliable binding constant to be extracted. However, a fluorescence titration performed by adding portions of the host cage to a  $10^{-5} \text{ M}$  solution of MAC showed that the MAC fluorescence is completely quenched as it is taken up into the cage (Figure 2), presumably by energy transfer from the excited state to the low-lying d–d states of the Co(II) ions. The 1:1 association constant determined from the fluorescence titration was  $2.0(2) \times 10^4 \text{ M}^{-1}$ .

To test the use of MAC in a fluorescence displacement assay, we performed experiments in which other guests, isoquinoline *N*-oxide (**1**) and adamantyl methyl ketone (**2**), were titrated into solutions containing a mixture of MAC and cage in water. Guest **1** is known to bind from previous work,<sup>12,13</sup> and guest **2** was identified by molecular modeling. As the competing guest increased in concentration and bound to the cage, MAC was displaced and the fluorescence at 443 nm increased in intensity (Figure 3). Fitting the fluorescence data to an isotherm that

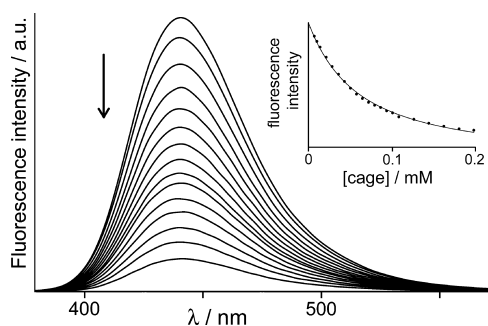


**Figure 2.** Fluorescence titration of MAC ( $10^{-5}$  M) with increasing amounts of cage in water at 298 K, showing progressive quenching of MAC as it binds in the cage cavity. Inset: best fit of the fluorescence intensity at 440 nm to a 1:1 binding isotherm.

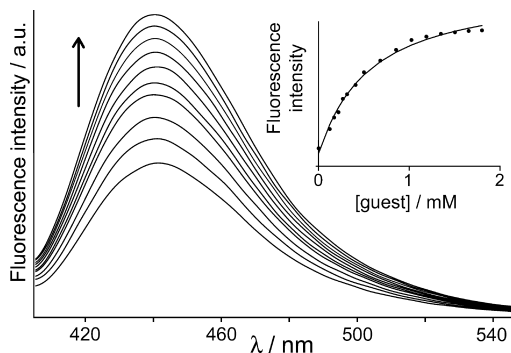


**Figure 3.** Restoration of fluorescence intensity from a MAC/cage mixture in water at 298 K (concentration of cage,  $5.7 \times 10^{-5}$  M; concentration of MAC,  $1.0 \times 10^{-5}$  M) by titration with isoquinoline-*N*-oxide (**1**), which displaces MAC from the cavity of the cage. Inset: best fit of the fluorescence intensity at 440 nm to a 1:1 binding isotherm.

considered the presence of two different 1:1 cage complexes gave association constants of  $4.0(3) \times 10^3 \text{ M}^{-1}$  for **1** and  $1.8(3) \times 10^4 \text{ M}^{-1}$  for **2**. These values are similar to the values measured by  $^1\text{H}$  NMR titrations:  $3.1(4) \times 10^3 \text{ M}^{-1}$  for **1**<sup>12</sup> and  $1.5(2) \times 10^4 \text{ M}^{-1}$  for **2** (this work). The assay was then optimized for use with a 384-well plate on a fluorescence plate reader (see the Experimental Section).

**(ii). Binding Studies on Aliphatic Ketones.** The automated fluorescence displacement assay was used to evaluate the 21 aliphatic ketones **3–23** shown in Scheme 1 as potential guests (Table 1; representative data sets from the assay are given in the Supporting Information). The carbonyl group confers water solubility and is a hydrogen-bond acceptor, which we have shown previously to be important for interactions with one of the two hydrogen-bond donor sites on the interior surface of the host.<sup>12</sup> The ketones feature a variety of different hydrophobic carbon cores of varying size and shape, providing a means of probing the internal dimensions of the host cavity. The results in Table 1 are discussed as two separate families of guests: **3–12** are a homologous series of cyclic aliphatic ketones of increasing ring size from  $\text{C}_5$  to  $\text{C}_{14}$ , which probe the overall capacity of the cavity (series A); **13–21** (and **8**) are a series of aliphatic ketones that have a  $\text{C}_{10}$  skeleton but different shapes and degrees of flexibility (series B). Guests **22** and **23** were used to test predictions about binding arising from measurements on series A. The largest compound in series A, **12**, was not sufficiently soluble in water even at micromolar levels for a

**Scheme 1**

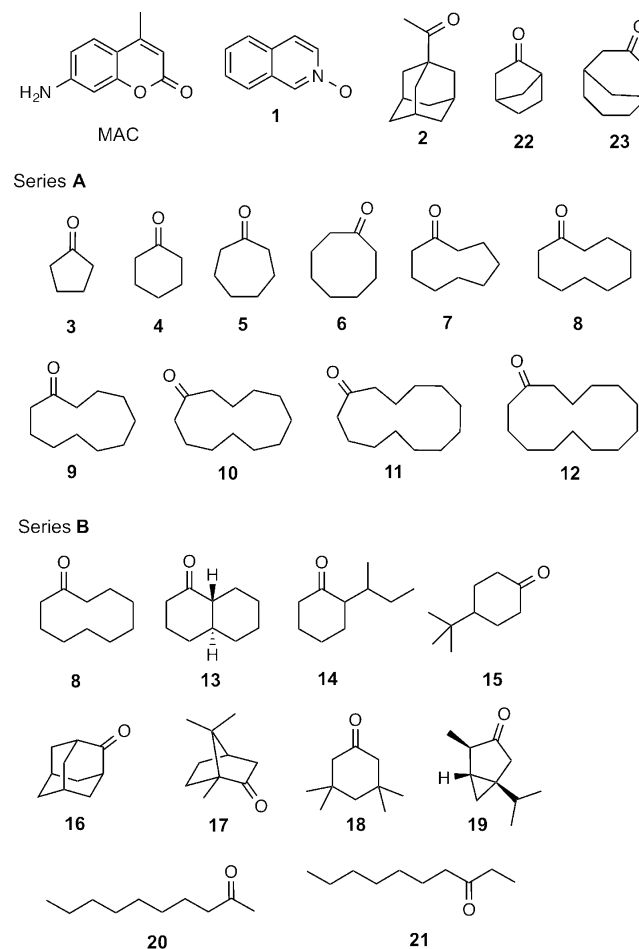


**Table 1. Binding Parameters (in Water at 298 K) and Shape Data for the Guests**

guest	$N_C$	$K/\text{M}^{-1}$	$-\Delta G^\circ/\text{kJ mol}^{-1}$	$V/\text{\AA}^3$	$SA/\text{\AA}^2$
<b>3</b> <sup>a</sup>	5	$1.3(2) \times 10^1$	6.3(4)	96	117
<b>4</b> <sup>b</sup>	6	$5.6(7) \times 10^1$	9.8(6)	115	133
<b>5</b>	7	$4.2(4) \times 10^2$	15.0(3)	133	150
<b>6</b>	8	$2.1(5) \times 10^3$	19.0(6)	150	165
<b>7</b>	9	$1.1(3) \times 10^4$	23.1(7)	169	183
<b>8</b>	10	$1.4(6) \times 10^5$	29(1)	186	198
<b>9</b>	11	$1.2(1) \times 10^6$	34.7(1)	205	212
<b>10</b>	12	$1.5(2) \times 10^5$	29.5(3)	224	238
<b>11</b>	13	$1.9(5) \times 10^4$	24.4(7)	242	255
<b>12</b>	14	too insoluble to measure		261	278
<b>13</b>	10	$9.5(10) \times 10^3$	22.7(3)	175	189
<b>14</b>	10	$1.6(1) \times 10^4$	24.0(2)	188	207
<b>15</b>	10	$8.7(20) \times 10^3$	22.5(6)	187	204
<b>16</b>	10	$1.9(1) \times 10^4$	24.4(1)	162	170
<b>17</b>	10	$1.8(3) \times 10^5$	30.0(4)	176	189
<b>18</b>	10	$7.5(20) \times 10^4$	27.8(7)	186	202
<b>19</b>	10	$2.0(1) \times 10^4$	24.5(1)	182	203
<b>20</b>	10	nb <sup>c</sup>	nb	202	234
<b>21</b>	10	nb <sup>c</sup>	nb	202	236
<b>22</b>	7	$1.3(3) \times 10^2$	12.1(6)	123	138
<b>23</b>	9	$4.00(4) \times 10^3$	20.5(1)	157	168

<sup>a</sup>Measured by NMR titration; this guest is in fast exchange on the NMR time scale. <sup>b</sup>Measured by NMR titration; this guest is in slow exchange on the NMR time scale. <sup>c</sup>nb = no binding detected.

reliable determination of  $K$ . For guests 5–19, 22, and 23, the binding constants were determined by the fluorescence displacement assay described above; the two most weakly binding guests from series A (3 and 4) required the higher concentrations accessible in  $^1\text{H}$  NMR titrations for reliable determination of the association constant. The series B guests 20 and 21 showed no evidence of binding in fluorescence or NMR titrations.

For the series A guests, the association constant increases steadily with the number of carbon atoms in the ring,  $N_C$ , up to cycloundecanone (9) ( $N_C = 11$ ;  $K = 1.2 \times 10^6 \text{ M}^{-1}$ ) and then drops by an order of magnitude for cyclododecanone (10) ( $N_C = 12$ ;  $K = 1.5 \times 10^5 \text{ M}^{-1}$ ) and again by another order of magnitude for cyclotridecanone (11) ( $N_C = 13$ ;  $K = 1.9 \times 10^4 \text{ M}^{-1}$ ) (Table 1). Molecular volume calculations indicate that the strongest-binding guest 9 has a volume of  $205 \text{ \AA}^3$ , equivalent to 50% of the host cavity volume, which lies in the range  $55 \pm 9\%$  noted by Rebek.<sup>2a,11</sup> (In fact, guest 10, whose volume is 55% of the cavity volume, appears to have a slightly more optimal size. However, we note that there is some uncertainty in the estimation of the cavity volume of the host due to the presence of the portals in the faces of the cubic assembly, so the values of the fractional occupancies of the guests are likewise subject to some uncertainty).

The relationship between the free energy change upon complexation,  $\Delta G^\circ$ , and the number of carbon atoms,  $N_C$ , for the series A ketones is shown in Figure 4. From 3 to 9,  $\Delta G^\circ$  is a

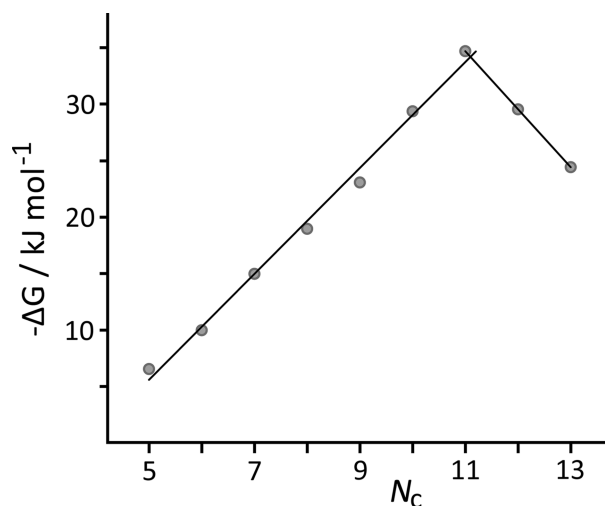


**Figure 4.** Plot of binding free energy vs number of C atoms for guest series A. The best-fit straight lines to the data points for  $N_C = 5$ –11 (rising:  $-\Delta G/\text{kJ mol}^{-1} = 4.7N_C - 18.1$ ;  $R^2 > 0.99$ ) and  $N_C = 11$ –13 (descending) are included.

linear function of  $N_C$  ( $R^2 > 0.99$ ), with each addition of a  $\text{CH}_2$  group stabilizing the complex by ca.  $5 \text{ kJ mol}^{-1}$  as a result of the increase in hydrophobic surface area (see below). For guests 9–11, we see a reversal of the previous trend, with a steady decrease in binding strength as the guests become increasingly too large. There are only three points in this series (12 was too insoluble for the assay), but the steady decrease in  $\Delta G^\circ$  with increasing steric bulk once the capacity of the host is exceeded is clear.

Figure 5 shows the relationship between the free energy change upon complexation,  $\Delta G^\circ$ , and the molecular surface area of the guest, SA. For the series A ketones 3–9 (i.e., before

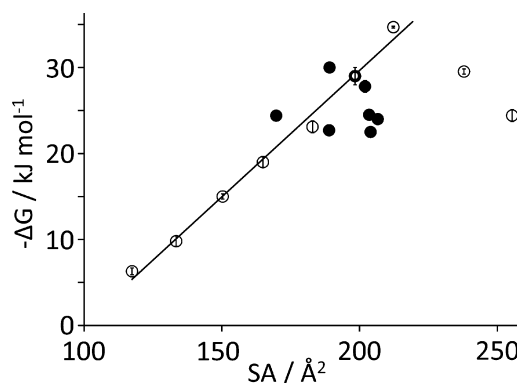


**Figure 5.** Plot of binding free energy vs guest surface area for guests in series A (○) and series B (●); guest 8 (○ with a thick border) is common to both sets. For series B, guests 20 and 21 do not bind and are not shown. In the region where there is a clear linear relationship for series A (guests 3–9), the best-fit straight line [ $-\Delta G/\text{kJ mol}^{-1} = 0.29(\text{SA}/\text{\AA}^2) - 29$ ;  $R^2 > 0.99$ ] is shown.

steric problems become important),  $\Delta G^\circ$  is a linear function of SA (open data points,  $R^2 > 0.99$ ), with a slope of  $0.3 \text{ kJ mol}^{-1} \text{ \AA}^{-2}$ . This value is consistent with previous correlations of the magnitude of the hydrophobic effect with burial of nonpolar surface area obtained from both biological and artificial systems.<sup>20</sup> For example, Fersht and co-workers showed that burial of methylene chains upon protein folding increased the stability by  $1.5(6) \text{ kcal mol}^{-1}$  per  $\text{CH}_2$  group, equating to ca.  $0.3 \text{ kJ mol}^{-1} \text{ \AA}^{-2}$ ,<sup>20j</sup> also, in a separate study using a range of alanine to glycine mutations at different positions on a protein, they derived a coefficient of  $0.055(3) \text{ kcal mol}^{-1} \text{ \AA}^{-2}$  (i.e.,  $0.23 \text{ kJ mol}^{-1} \text{ \AA}^{-2}$ ) for the change in stability associated with a change in hydrophobic surface area.<sup>20g</sup> In nonbiological systems, experimental data on the free energy of transfer of alkanes from water to *n*-hexadecane shows that each additional  $\text{CH}_2$  group in the solute decreases the free energy of phase transfer by  $3.6 \text{ kJ mol}^{-1}$ , which equates to  $0.2 \text{ kJ mol}^{-1}$  per square angstrom of solute molecular surface area.<sup>15g</sup> When a guest binds inside the cage cavity, not only is the guest transferred from an aqueous environment to a hydrocarbon environment, but the internal surface of the cage is also desolvated to make contact with the guest hydrocarbon surface. Thus, the maximum possible free energy contribution to binding is expected to be double that for the free energy of phase transfer; that is, complete desolvation of an alkane guest in an alkane cavity that makes optimal contact with the entire surface of the guest would be expected to result in a stabilization of the complex of  $0.4 \text{ kJ mol}^{-1} \text{ \AA}^{-2}$ .<sup>15g,19</sup> The observed stabilization of  $0.3 \text{ kJ mol}^{-1} \text{ \AA}^{-2}$  in the cage complexes (Figure 5) is somewhat less than this, consistent with the fact that the internal surface of the cage is significantly more polar than an alkane, as shown by its ability to act as a hydrogen-bond donor.<sup>12</sup>

We can consider the guests to be composed of a nonpolar (hydrocarbon) region and a polar (carbonyl) region. The surface areas of the series A guests can be described by eq 1, which is the best-fit straight line to the graph of SA versus  $N_{\text{CH}_2}$ , the number of  $\text{CH}_2$  groups in the guest (see the Supporting Information):

$$\text{SA}/\text{\AA}^2 = 54 + 16N_{\text{CH}_2} \quad (1)$$



The constant,  $54 \text{ \AA}^2$ , represents the surface area of the carbonyl group, and each  $\text{CH}_2$  group adds a surface area of  $16 \text{ \AA}^2$ . We can use eq 1 to define the total surface area of the  $\text{CH}_2$  groups,  $\text{SA}_{\text{CH}_2}$  (eq 2).

$$\text{SA}_{\text{CH}_2}/\text{\AA}^2 = \text{SA}/\text{\AA}^2 - 54 \quad (2)$$

Combining eq 2 with the line of best fit to the  $-\Delta G^\circ$  versus SA data shown in Figure 5 gives eq 3:

$$\Delta G^\circ/\text{kJ mol}^{-1} = 13 - 0.3(\text{SA}_{\text{CH}_2}/\text{\AA}^2) \quad (3)$$

The second term on the right-hand side represents the favorable hydrophobic contribution to guest binding associated with the  $\text{CH}_2$  groups, as discussed above. The first term is a constant unfavorable contribution of  $13 \text{ kJ mol}^{-1}$  to the change in free energy upon complexation due to binding of the polar carbonyl group. The unfavorable free energy change associated with the formation of a bimolecular complex in solution is  $6 \text{ kJ mol}^{-1}$ ,<sup>21</sup> which implies that binding of the carbonyl group in the cage is associated with an unfavorable free energy change of  $7 \text{ kJ mol}^{-1}$ . This adverse free energy change reflects the thermodynamic cost of desolvation of the carbonyl oxygen upon its removal from water, for which the formation of weaker interactions with the CH groups in the polar binding site inside the cage does not fully compensate.

The second series of guests (series B: **8** and **13–21**) are all  $\text{C}_{10}$  ketones with similar volumes ( $162\text{--}202 \text{ \AA}^3$ ) and surface areas ( $170\text{--}236 \text{ \AA}^2$ ) but different shapes. In this case, there is no simple correlation between  $\Delta G^\circ$  and SA (solid circles in Figure 5). Comparison of the parent series A cyclohexanone (**4**) with the three isomeric substituted series B cyclohexanones **14**, **15**, and **18** is instructive. Whereas **4** binds weakly ( $K = 58 \text{ M}^{-1}$ ), **14**, **15**, and **18** all bind with much higher affinities ( $K = 16\,000$ ,  $8\,700$ , and  $75\,000 \text{ M}^{-1}$ , respectively). The higher binding affinity of the substituted compounds is due to the increase in nonpolar surface area (an additional ca.  $70 \text{ \AA}^2$  in each case), which means that the larger guests are better able to fill the cavity and form favorable hydrophobic interactions with the interior surface of the cage. However, the association constants for **14**, **15**, and **18** span an order of magnitude, even though these compounds have similar molecular volumes and surface areas. These guests are close to the limiting volume that the cage can accommodate, so small changes in structure have a large effect on the binding affinity.<sup>12</sup> The most symmetrical guest, dislike **18**, fits best into the cavity in the cage, whereas the unsymmetrical shape of **14** and the elongated shape of **15** make them slightly less complementary guests, presumably because of adverse steric interactions with the walls of the cavity. Similarly, comparison of **8** and its more rigid bicyclic analogue **13** shows how rigidification of a guest can have a detrimental effect on binding, as **13** is a poorer shape match for the cavity than disc-shaped **8**.

The two acyclic ketones **20** and **21** show no detectable binding ( $K < 1 \text{ M}^{-1}$ ). These molecules can adapt to any shape required to bind inside the cage, and the fact that cyclic ketones with similar molecular volumes bind strongly suggests that the size and shape of the cavity should not present a problem for the acyclic guests. However, there are both enthalpic and entropic penalties associated with reorganizing these compounds to fit inside the cage. The lowest-energy conformations of **20** and **21** are extended with all of the carbon–carbon bonds in a staggered conformation, and these bonds must adopt high-energy gauche conformations to fold the molecules up into

compact structures that will fit inside the cage.<sup>22</sup> In addition, **20** and **21** are conformationally flexible and can adopt a significantly larger number of conformations in solution than inside the cage, so there is an entropic penalty associated with reducing the size of the conformational ensemble upon binding.

Comparison of the strong correlation of  $\Delta G^\circ$  with SA within series A (as far as guest **9** but not beyond) with the absence of any correlation of  $\Delta G^\circ$  with SA for series B clearly shows the limits within which we can predict with confidence the binding strengths of other guests of the aliphatic ketone family. To test this, we evaluated guests **22** and **23** whose bicyclic nature gives them surface area/volume values that lie between the limits of the linear correlation region of series A but do not exactly match any members of the series. From the trend line shown in Figure 5 and the calculated surface areas of **22** and **23**, we can predict  $\Delta G^\circ$  values for binding of  $-11.7$  and  $-20.3 \text{ kJ/mol}$ , which translate to predicted association constants of  $110$  and  $3600 \text{ M}^{-1}$ , respectively. These are in excellent agreement with the measured values determined using the fluorescence displacement assay (Table 1).

(iii). **Crystal Structure of a Complex.** An X-ray crystal structure of the complex with guest **9** (the most strongly binding of the guests we investigated) bound inside the cage is shown in Figures 6–8. We found that growing crystals from solvents containing excess guest afforded only the empty cage, whose structure we reported recently.<sup>13</sup> However, immersing preformed crystals of the cage in neat cycloundecanone (containing a drop of methanol to prevent desolvation of the crystals) resulted in uptake of the guest without damaging the crystals. This technique has been used by others to characterize guest species in the cavities of porous coordination networks and other inclusion compounds, which in many cases can retain their crystallinity following reversible uptake/release of guests in the solid state.<sup>23</sup>

The conformation of the cage is not affected by the presence of the guest, which is disordered over two symmetrically equivalent orientations (only one is shown). The oxygen atom of the guest carbonyl group was straightforward to identify in the electron density map on the basis of the polar interactions with well-defined sites on the interior surface of the cage that hold it in place (see below), but the carbon atoms required geometric restraints to allow the construction of a reasonable model that gave a stable refinement.

The disc-shaped guest is located centrally in the cavity with the carbonyl group projected toward one of the two regions of high positive electrostatic potential associated with the *fac* trischelate sites, which lie at either end of the long diagonal of the cube (Figures 6 and 7). These are the regions where several CH protons from methylene and naphthyl groups converge to form a binding pocket for hydrogen-bond-acceptor guests.<sup>12,13,24</sup> The carbonyl oxygen makes short contacts of between  $2.54$  and  $3.06 \text{ \AA}$  with four CH protons in this pocket (Figure 7). The  $\text{Co}\cdots\text{O}$  separation in this site is  $5.72 \text{ \AA}$ , which is similar to that observed for solvent molecules that occupy this position in other crystal structures.<sup>12,13,24</sup> Previous work suggests that these interactions contribute significantly to binding in organic solvents<sup>12</sup> but make little contribution to the binding affinity in water because the formation of  $\text{CH}\cdots\text{O}$  interactions between the cage and the guest requires displacement of water  $\text{OH}\cdots\text{O}$  and  $\text{CH}\cdots\text{O}$  interactions.<sup>13</sup> However, these polar interactions are important in determining the orientation of the guest, and the presence of two *fac* trischelate sites in the cavity accounts for the two degenerate binding

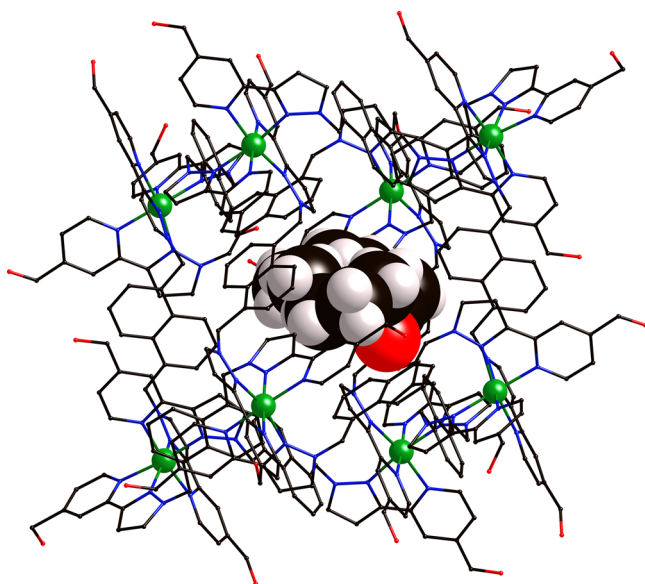


**Figure 6.** View of the X-ray crystal structure of the cage·9 complex,  $[\text{Co}_8\text{L}_{12}\cdot(9)](\text{BF}_4)_{16}$ . The  $[\text{Co}_8\text{L}_{12}]^{16+}$  complex cation is shown in wireframe mode and the guest in space-filling mode.

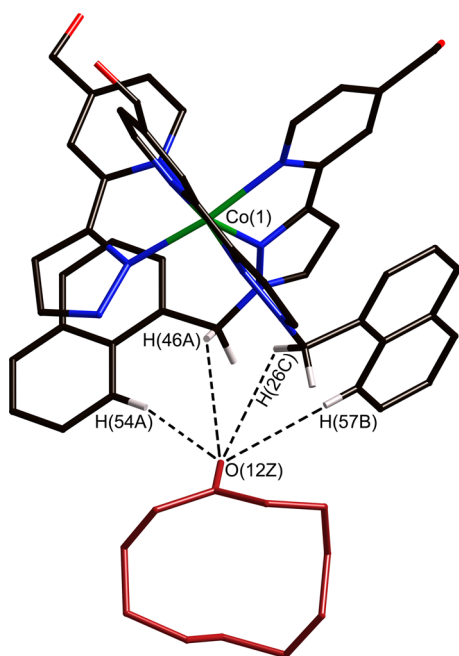


**Figure 7.** Close-up view of the crystal structure showing the closest contacts between the carbonyl group of **9** and some of the naphthyl and methylene CH protons of the cage (see the main text).

modes found for **9** in the crystal structure (the alternate disordered component of guest **9** is symmetrically equivalent by inversion across the center of the cavity, oriented such that it interacts with the structurally identical binding pocket at the other end of the long diagonal). Figure 8, which displays a slice through the center of the structure in space-filling mode with the guest colored in green, shows that **9** does not completely fill the cavity of the cage; it makes contact with the cage surface around its “equator” but there is space on either face of the guest disc where contact with the cage is poorer. Thus, there is a slight mismatch between the shapes of the pseudospherical cavity and the disc-shaped guest; a more spherical guest that

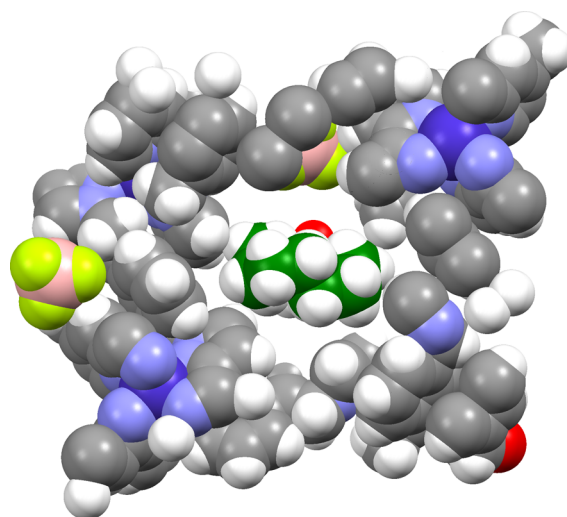


**Figure 8.** Slice through a space-filling model of the crystal structure of  $[\text{Co}_8\text{L}_{12}\cdot(9)](\text{BF}_4)_{16}$  illustrating the extent to which guest **9** fills the cavity of the host.

would make better contact with all of the cage internal surface would therefore be expected to bind even more strongly. The conformation of **9** bound inside the cage is very similar to the minimum-energy conformation calculated for **9** in vacuo (Figure 9), indicating that **9** is almost perfectly preorganized for guest binding.

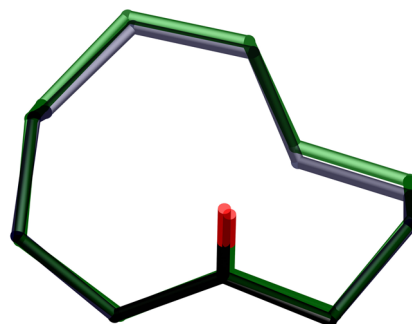


**Figure 9.** Superimposition the calculated minimum-energy conformation of **9** in vacuo (green bonds) and the observed conformation in the X-ray crystal structure of the cage·9 complex (dark-blue bonds).

## CONCLUSIONS

The development of a new fluorescence displacement assay for a water-soluble host cage has allowed a wide series of aliphatic ketones to be evaluated as guests in a systematic and quantitative study of guest binding in a coordination cage host. As the binding is dominated by hydrophobic effects, we have observed many examples of very strong binding, with the highest-affinity guest being cycloundecanone (**9**) ( $K = 1.2 \times 10^6 \text{ M}^{-1}$ ), which has an association constant 2–3 orders of magnitude higher than those of the more polar guests we examined previously.<sup>13</sup> This complex has been structurally characterized and shows how (i) the alkyl backbone of the disc-shaped guest forms close contacts with the interior surface of the cavity and (ii) the carbonyl group is directed into the pocket at one of the two *fac* trischelate vertices that provide hydrogen-bond donor sites on the internal surface of the host.

The two series of guests studied show quite different behaviors: the observations within each series are interesting in themselves, but the difference between the two series is also noteworthy. With guests in series A, as long as the point where steric bulk becomes limiting is not reached, we see an excellent correlation between binding affinity and guest size. In particular, increments in guest binding affinity across the series are consistent with expectations based on the increased hydrophobic surface area. The peak is reached with guest **9**, which fills 50% of the volume of the host cavity, close to the optimal guest volume of  $55 \pm 9\%$  noted by Rebek.<sup>2a,11</sup> Binding decreases beyond this, presumably for simple steric reasons.

In contrast, with series B there is no such simple correlation between surface area and binding affinity. As these guests (all  $C_{10}$ ) are close to the size limit that the cage cavity can accommodate, steric issues become dominant, with variations in shape and substitution pattern becoming more important than the relatively minor changes in hydrophobic surface area or molecular volume among a family of guests of generally similar bulk. Comparisons of **8** and **13** and of the three isomeric substituted cyclohexanones **14**, **15**, and **18** show how guests with more eccentric shapes are poorer fits for the pseudospherically symmetric cavity. The linear ketones **20** and **21** do not bind at all, which we ascribe to the enthalpy and entropy costs associated with the substantial conformational reorganization that would be required.

Thus, within certain limits, we can predict guest binding very well on the basis of the correlation between  $\Delta G^\circ$  and guest surface area. These limits are that (i) the guests need to be preorganized to the extent of being at least monocyclic and (ii) the guests need to be small enough for steric limitations on binding not to be an issue.

## EXPERIMENTAL SECTION

The host cage  $[\text{Co}_8\text{L}_{12}](\text{BF}_4)_{16}$  was prepared according to the published method.<sup>13</sup> All of the ketone guests were commercially available from Sigma-Aldrich and used as received. <sup>1</sup>H NMR spectra were recorded on a Bruker Avance-III 400 MHz instrument.

The fluorescence displacement assay was carried out by preparing a stock solution of MAC (0.01 mM) and cage (0.04 mM) in distilled water. A 10 mL sample of the guest under investigation at a higher known concentration (0.85–12.0 mM) was made using the MAC/cage stock solution. To 12–24 wells of a Griener Bio-one  $\mu$ Clear black 384-well plate were added aliquots of the MAC/cage stock solution (0–100  $\mu\text{L}$ ) and the guest solution (0–100  $\mu\text{L}$ ) in different proportions to a total volume of 100  $\mu\text{L}$  in each well. The fluorescence emission at 450 nm (using 400 nm excitation to avoid the competing absorption by ligands in the cage) was measured for each well using a BMG FLUOstar Omega plate reader equilibrated at 298 K. From the known value of the cage-MAC association constant ( $2.0 \times 10^4 \text{ M}^{-1}$ ), changes in fluorescence emission were fit in Microsoft Excel to an isotherm that allowed for the presence of two competing 1:1 complexes to obtain the association constant for guest binding. Each titration was repeated at least three times, and the experimental error is quoted as twice the standard deviation at a precision of one significant figure.

The gas-phase minimum-energy conformation of **9** (Figure 9) was calculated using a conformational search in Macromodel<sup>25</sup> with the MMFF force field. Molecular volumes and surface areas were calculated from the 0.002 bohr  $\text{\AA}^{-3}$  isodensity surface obtained by B3LYP 6-31G\* density functional theory calculations implemented in Spartan.<sup>26</sup>

The crystal structure of the complex  $[\text{Co}_8\text{L}_{12}(\mathbf{9})](\text{BF}_4)_{16}$  was obtained at the EPSRC National Crystallography Service at the University of Southampton, UK.<sup>27</sup> Crystallographic data are as follows:  $[\text{Co}_8\text{L}_{12}](\text{BF}_4)_{16}$  (cycloundecanone):  $C_{371}H_{330}B_{16}Co_8F_{64}N_{72}O_{25}$ ,  $M =$

8057.5 g/mol; monoclinic, space group  $C2/c$ ;  $a = 27.5037(19) \text{ \AA}$ ,  $b = 39.282(3) \text{ \AA}$ ,  $c = 42.103(3) \text{ \AA}$ ,  $\beta = 106.2580(10)^\circ$ ,  $V = 43440(5) \text{ \AA}^3$ ,  $Z = 4$ ;  $\rho_{\text{calc}} = 1.232 \text{ g cm}^{-3}$ ,  $T = 100(2) \text{ K}$ ,  $\lambda(\text{Mo K}\alpha) = 0.71073 \text{ \AA}$ ,  $\mu = 0.388 \text{ mm}^{-1}$ ; 129 875 reflections with  $2\theta_{\text{max}} = 50^\circ$  were merged to give 38 209 independent reflections ( $R_{\text{int}} = 0.0712$ ); final  $R_1$  [for data with  $I > 2\sigma(I)$ ] = 0.187,  $wR_2$  (all data) = 0.525. The structure was solved and refined using the SHELX suite of programs.<sup>28</sup> The asymmetric unit contains one-half of the cage complex, which lies astride an inversion center, as well as one complete guest molecule, whose atoms all have site occupancies of 0.5. Thus, the complete complex contains one guest molecule disordered over two symmetrically equivalent (and spatially overlapping) orientations with the O atom pointing toward diagonally opposite corners Co(1) and Co(1A). The usual disorder of anions/solvent molecules and solvent loss characteristic of cage complexes of this type resulted in weak scattering, necessitating use of extensive geometric and displacement restraints to keep the refinement stable; these are described in detail in the CIF provided in the Supporting Information. We could locate and refine five of the expected eight  $[\text{BF}_4]^-$  anions in the asymmetric unit. The presence of large regions of diffuse electron density that could not be modeled, accounting for the remaining anions plus solvent molecules, required use of the "Solvent Mask" function in the OLEX-2 software package.<sup>29</sup> The thermal displacement parameters of the atoms of the guest molecule in the cage cavity are larger than those of the rest of the cage structure. This could arise from unresolved positional disorder or from the fact that the fraction of cage cavities occupied by guest molecules is less than 100%. We assumed the former explanation and left the site occupancies at 0.5 for each disordered component for the final refinement (i.e., one complete guest molecule per host cage). Overall, the final  $R_1$  value of 18.7% is typical of cage structures of this type and is sufficient to establish the identity and connectivity of the complex.

## ASSOCIATED CONTENT

### Supporting Information

Titration data used to determine binding constants; additional graphs of SA vs  $N_{\text{CH}_3}$  and  $\Delta G^\circ$  vs  $\text{SA}_{\text{CH}_3}$  used to derive eqs 1 and 3; and crystallographic data in CIF format. This material is available free of charge via the Internet at <http://pubs.acs.org>. The crystallographic data can also be obtained free of charge from The Cambridge Crystallographic Data Centre via [www.ccdc.cam.ac.uk/data\\_request/cif](http://www.ccdc.cam.ac.uk/data_request/cif).

## AUTHOR INFORMATION

### Corresponding Authors

[c.hunter@sheffield.ac.uk](mailto:c.hunter@sheffield.ac.uk)  
[m.d.ward@sheffield.ac.uk](mailto:m.d.ward@sheffield.ac.uk)

### Notes

The authors declare no competing financial interest.

## ACKNOWLEDGMENTS

We thank the EPSRC for financial support.

## REFERENCES

- (1) Reviews of coordination cages: (a) Fiedler, D.; Leung, D. H.; Bergman, R. G.; Raymond, K. N. *Acc. Chem. Res.* **2005**, *38*, 349. (b) Fujita, M.; Tominaga, M.; Hori, A.; Therrien, B. *Acc. Chem. Res.* **2005**, *38*, 369. (c) Seidel, S. R.; Stang, P. J. *Acc. Chem. Res.* **2002**, *35*, 972. (d) Hamilton, T. D.; MacGillivray, L. R. *Cryst. Growth Des.* **2004**, *4*, 419. (e) Ward, M. D. *Chem. Commun.* **2009**, 4487. (f) Perry, J. J.; Perman, J. A.; Zaworotko, M. J. *Chem. Soc. Rev.* **2009**, *38*, 1400. (g) Alvarez, S. *Dalton Trans.* **2006**, 2209. (h) Amouri, H.; Desmarets, C.; Moussa, J. *Chem. Rev.* **2012**, *112*, 2015. (i) Williams, A. F. *Coord. Chem. Rev.* **2011**, *255*, 2104. (j) Laughrey, Z.; Gibb, B. C. *Chem. Soc. Rev.* **2011**, *40*, 363. (k) Jin, P.; Dalgarno, S. J.; Atwood, J. L. *Coord. Chem. Rev.* **2012**, *254*, 1760. (l) Chakrabarty, R. J.; Mukherjee, P. S.; Stang, P. J. *Chem. Rev.* **2011**, *111*, 6810. (m) Inokuma, Y.; Kawano, M.;



Fujita, M. *Nat. Chem.* **2011**, *3*, 349. (n) Pluth, M. D.; Bergman, R. G.; Raymond, K. N. *Acc. Chem. Res.* **2009**, *42*, 1650. (o) Breiner, B.; Clegg, J. K.; Nitschke, J. R. *Chem. Sci.* **2011**, *2*, 51. (p) Smulders, M. M. J.; Riddell, I. A.; Browne, C.; Nitschke, J. R. *Chem. Soc. Rev.* **2013**, *42*, 1728. (q) Nakamura, T.; Ube, H.; Shionoya, M. *Chem. Lett.* **2014**, *42*, 328.

(2) Reviews of organic capsules: (a) Rebek, J., Jr. *Acc. Chem. Res.* **2009**, *42*, 1660. (b) Cram, D. J. *Angew. Chem., Int. Ed. Engl.* **1988**, *27*, 1009. (c) Rieth, S.; Hermann, K.; Wang, B.-Y.; Badjić, J. *Chem. Soc. Rev.* **2011**, *40*, 1609. (d) Hof, F.; Craig, S. L.; Nuckolls, C.; Rebek, J., Jr. *Angew. Chem., Int. Ed.* **2002**, *41*, 1488. (e) Hooley, R. J.; Rebek, J., Jr. *Chem. Biol.* **2009**, *16*, 255. (f) Purse, B. W.; Rebek, J., Jr. *Proc. Natl. Acad. Sci. U.S.A.* **2005**, *102*, 10777. (g) Cram, D. J. *Nature* **1992**, *356*, 29. (h) Yoshizawa, M.; Klosterman, J. *Chem. Soc. Rev.* **2014**, *43*, 1885. (i) Collet, A.; Dutasta, J.-P.; Lozach, B.; Canceill, J. *Top. Curr. Chem.* **1993**, *165*, 103. (j) Conn, M. M.; Rebek, J., Jr. *Chem. Rev.* **1997**, *97*, 1647. (k) Sherman, J. C. *Tetrahedron* **1995**, *51*, 3395. (l) Ajami, D.; Rebek, J., Jr. *Acc. Chem. Res.* **2013**, *46*, 990. (m) Adriaenssens, L.; Ballester, P. *Chem. Soc. Rev.* **2013**, *42*, 3261.

(3) Host–guest chemistry in cage complexes: (a) Clever, G. H.; Kawamura, W.; Tashiro, S.; Shiro, M.; Shionoya, M. *Angew. Chem., Int. Ed.* **2012**, *51*, 2606. (b) Han, M.; Hey, J.; Kawamura, W.; Stalke, D.; Shionoya, M. *Inorg. Chem.* **2012**, *51*, 9574. (c) Clever, G. H.; Tashiro, S.; Shionoya, M. *J. Am. Chem. Soc.* **2010**, *132*, 9973. (d) Harris, K.; Fujita, D.; Fujita, M. *Chem. Commun.* **2013**, *49*, 6703. (e) Browne, C.; Brenet, S.; Clegg, J. K.; Nitschke, J. R. *Angew. Chem., Int. Ed.* **2013**, *52*, 1944. (f) Mal, P.; Breiner, B.; Rissanen, K.; Nitschke, J. R. *Science* **2009**, *324*, 1697. (g) Yoshizawa, M.; Kusukawa, T.; Fujita, M.; Sakamoto, S.; Yamaguchi, K. *J. Am. Chem. Soc.* **2001**, *123*, 10454. (h) Lewis, J. E. M.; Gavey, E. L.; Cameron, S. A.; Crowley, J. D. *Chem. Sci.* **2012**, *3*, 778. (i) Yi, J. W.; Barry, N. P. E.; Furrer, M. A.; Zava, O.; Dyson, P. J.; Therrien, B.; Kim, B. H. *Bioconjugate Chem.* **2012**, *23*, 461. (j) Amouri, H.; Mimassi, L.; Rager, M. N.; Mann, B. E.; Guyard-Duhayon, C.; Raehm, L. *Angew. Chem., Int. Ed.* **2005**, *44*, 4543. (k) Desmarest, C.; Contard, G.; Cooksy, A. L.; Rager, M. N.; Amouri, H. *Inorg. Chem.* **2014**, *53*, 4287.

(4) Catalysis in cage complexes: (a) Hastings, C. J.; Fiedler, D.; Bergman, R. G.; Raymond, K. N. *J. Am. Chem. Soc.* **2008**, *130*, 10977. (b) Brown, C. J.; Bergman, R. G.; Raymond, K. N. *J. Am. Chem. Soc.* **2009**, *131*, 17530. (c) Hastings, C. J.; Pluth, M. D.; Bergman, R. G.; Raymond, K. N. *J. Am. Chem. Soc.* **2010**, *132*, 6938. (d) Yoshizawa, M.; Tamura, M.; Fujita, M. *Science* **2006**, *312*, 251. (e) Nishioka, Y.; Yamaguchi, T.; Yoshizawa, M.; Fujita, M. *J. Am. Chem. Soc.* **2007**, *129*, 7000. (f) Horiuchi, S.; Murase, T.; Fujita, M. *Chem.—Asian J.* **2011**, *6*, 1839. (g) Bolliger, J. L.; Berlunguer, A. M.; Nitschke, J. R. *Angew. Chem., Int. Ed.* **2013**, *52*, 7958. (h) Kopilevich, S.; Gil, A.; Garcia-Rates, M.; Bonet-Avalos, J.; Bo, C.; Müller, A.; Weinstock, I. A. *J. Am. Chem. Soc.* **2012**, *134*, 13082.

(5) Guest binding in organic capsules: (a) Moerkerke, S.; Le Gac, S.; Topić, F.; Rissanen, K.; Jabin, I. *Eur. J. Org. Chem.* **2013**, 5315. (b) Slovak, S.; Cohen, Y. *Chem.—Eur. J.* **2012**, *18*, 8515. (c) Corbellini, F.; Di Costanzo, L.; Crego-Calama, M.; Geremia, S.; Reinhoudt, D. N. *J. Am. Chem. Soc.* **2003**, *125*, 9946. (d) Ajami, D.; Tolstoy, P. M.; Dube, H.; Odermatt, S.; Koeppe, B.; Guo, J.; Limbach, H.-H.; Rebek, J., Jr. *Angew. Chem., Int. Ed.* **2011**, *50*, 528. (e) Kerckhoffs, J. M. C. A.; ten Cate, M. G. J.; Mateos-Timoneda, M. A.; van Leeuwen, F. W. B.; Snellink-Ruël, B.; Spek, A. L.; Kooijman, H.; Crego-Calama, M.; Reinhoudt, D. N. *J. Am. Chem. Soc.* **2005**, *127*, 12697. (f) Shenoy, S. R.; Crisostomo, F. R. P.; Iwasawa, T.; Rebek, J., Jr. *J. Am. Chem. Soc.* **2008**, *130*, 5658. (g) Ichihara, H.; Kawai, H.; Togari, Y.; Kikuta, E.; Kitagawa, H.; Tsuzuki, S.; Yoza, K.; Yamanaka, M.; Kobayashi, K. *Chem.—Eur. J.* **2013**, *19*, 3685. (h) Cram, D. J.; Tanner, M. E.; Thomas, R. *Angew. Chem., Int. Ed. Engl.* **1991**, *30*, 1024. (i) Galan, A.; Gil-Ramirez, G.; Ballester, P. *Org. Lett.* **2013**, *15*, 4976.

(6) Clever, G. H.; Tashiro, S.; Shionoya, M. *Angew. Chem., Int. Ed.* **2009**, *48*, 7010.

(7) Custelcean, R.; Bonnesen, P. V.; Duncan, N. C.; Zhang, X.; Watson, L. A.; Van Berkel, G.; Parson, W. B.; Hay, B. P. *J. Am. Chem. Soc.* **2012**, *134*, 8525.

(8) (a) Kishi, N.; Li, Z.; Yoza, K.; Akita, M.; Yoshizawa, M. *J. Am. Chem. Soc.* **2011**, *133*, 11438. (b) Sawada, T.; Fujita, M. *J. Am. Chem. Soc.* **2010**, *132*, 7194. (c) Ronson, T. K.; Giri, C.; Beyeh, N. K.; Minkkinen, A.; Topić, F.; Holstein, J. J.; Rissanen, K.; Nitschke, J. R. *Chem.—Eur. J.* **2013**, *19*, 3374. (d) Samanta, D.; Mukherjee, S.; Patil, Y. P.; Mukherjee, P. S. *Chem.—Eur. J.* **2012**, *18*, 12322. (e) Barry, N. P. E.; Zava, O.; Wu, W.; Zhao, J. Z.; Therrien, B. *Inorg. Chem. Commun.* **2012**, *18*, 25. (f) Hatakeyama, Y.; Sawada, T.; Kawano, M.; Fujita, M. *Angew. Chem., Int. Ed.* **2009**, *48*, 8695. (g) Brumaghim, J. L.; Michels, M.; Raymond, K. N. *Eur. J. Org. Chem.* **2004**, 4552.

(9) (a) Kishi, N.; Li, Z.; Sei, Y.; Akita, M.; Yoza, K.; Siegel, J. S.; Yoshizawa, M. *Chem.—Eur. J.* **2013**, *19*, 6313. (b) Murase, T.; Otsuka, K.; Fujita, M. *J. Am. Chem. Soc.* **2010**, *132*, 7864. (c) Yamauchi, Y.; Yoshizawa, M.; Akita, M.; Fujita, M. *J. Am. Chem. Soc.* **2010**, *132*, 960. (d) Yoshizawa, M.; Nakagawa, J.; Kurnazawa, K.; Nagao, M.; Kawano, M.; Ozeki, T.; Fujita, M. *Angew. Chem., Int. Ed.* **2005**, *44*, 1810. (e) Therrien, B. *Chem.—Eur. J.* **2013**, *19*, 8378.

(10) Smulders, M. M. J.; Zarra, S.; Nitschke, J. R. *J. Am. Chem. Soc.* **2013**, *135*, 7039.

(11) (a) Ams, M. R.; Ajami, D.; Craig, S. L.; Yang, J. S.; Rebek, J., Jr. *J. Am. Chem. Soc.* **2009**, *131*, 13190. (b) Mecozzi, S.; Rebek, J., Jr. *Chem.—Eur. J.* **1998**, *4*, 1016.

(12) (a) Turega, S.; Whitehead, M.; Hall, B. R.; Haddow, M. F.; Hunter, C. A.; Ward, M. D. *Chem. Commun.* **2012**, *48*, 2752. (b) Turega, S.; Whitehead, M.; Hall, B. R.; Meijer, A. J. H. M.; Hunter, C. A.; Ward, M. D. *Inorg. Chem.* **2013**, *52*, 1122.

(13) Whitehead, M.; Turega, S.; Stephenson, A.; Hunter, C. A.; Ward, M. D. *Chem. Sci.* **2013**, *4*, 2744.

(14) (a) Ward, M. D. *Chem. Commun.* **2009**, 4487. (b) Tidmarsh, I. S.; Faust, T. B.; Adams, H.; Harding, L. P.; Russo, L.; Clegg, W.; Ward, M. D. *J. Am. Chem. Soc.* **2008**, *130*, 15167.

(15) (a) Southall, N. T.; Dill, K. A.; Haymet, A. D. J. *J. Phys. Chem. B* **2002**, *106*, 521. (b) Hummer, G.; Garde, S.; Garcia, A. E.; Paulaitis, M. E.; Pratt, L. R. *J. Phys. Chem. B* **1998**, *102*, 10469. (c) Pratt, L. R.; Pohorille, A. *Chem. Rev.* **2002**, *102*, 2671. (d) Tanford, C. *Science* **1978**, *200*, 1012. (e) Houk, K. N.; Leach, A. G.; Kim, S. P.; Zhang, X. *Angew. Chem., Int. Ed.* **2003**, *42*, 4872. (f) Meyer, E. A.; Castellano, R. K.; Diederich, F. *Angew. Chem., Int. Ed.* **2003**, *42*, 1210. (g) Hunter, C. A. *Chem. Sci.* **2013**, *4*, 834.

(16) (a) Hunter, C. A.; Misuraca, M. C.; Turega, S. M. *J. Am. Chem. Soc.* **2011**, *133*, 582. (b) Jinks, M. A.; Sun, H.; Hunter, C. A. *Org. Biomol. Chem.* **2014**, *12*, 1440. (c) Hunter, C. A.; Misuraca, M. C.; Turega, S. M. *Chem. Sci.* **2012**, *3*, 589. (d) Chekmeneva, E.; Hunter, C. A.; Misuraca, M. C.; Turega, S. M. *Org. Biomol. Chem.* **2012**, *10*, 6022. (e) Adams, H.; Chekmeneva, E.; Hunter, C. A.; Misuraca, M. C.; Navarro, C.; Turega, S. M. *J. Am. Chem. Soc.* **2013**, *135*, 1853. (f) Hunter, C. A.; Misuraca, M. C.; Turega, S. M. *Chem. Sci.* **2012**, *3*, 2462. (g) Hunter, C. A.; Misuraca, M. C.; Turega, S. M. *J. Am. Chem. Soc.* **2011**, *133*, 20416. (h) Buurma, N. J.; Cook, J. L.; Hunter, C. A.; Low, C. M. R.; Vinter, J. G. *Chem. Sci.* **2010**, *1*, 242. (i) Amenta, V.; Cook, J. L.; Hunter, C. A.; Low, C. M. R.; Vinter, J. G. *Org. Biomol. Chem.* **2011**, *9*, 7571. (j) Amenta, V.; Cook, J. L.; Hunter, C. A.; Low, C. M. R.; Vinter, J. G. *J. Phys. Chem. B* **2012**, *116*, 14433. (k) Amenta, V.; Cook, J. L.; Hunter, C. A.; Low, C. M. R.; Sun, H.; Vinter, J. G. *J. Am. Chem. Soc.* **2013**, *135*, 12091.

(17) (a) Nau, W. M.; Ghale, G.; Hennig, A.; Bakirci, H.; Bailey, D. M. *J. Am. Chem. Soc.* **2009**, *131*, 11558. (b) Comby, S.; Tuck, S. A.; Truman, L. K.; Kotova, O.; Gunnlaugsson, T. *Inorg. Chem.* **2012**, *51*, 10158. (c) Vannoy, C. H.; Chong, L.; Le, C.; Krull, U. J. *Anal. Chim. Acta* **2013**, *759*, 92. (d) Chang, J. C.; Tomlinson, I. D.; Warnement, M. R.; Iwamoto, H.; DeFelice, L. J.; Blakely, R. D.; Rosenthal, S. J. *J. Am. Chem. Soc.* **2011**, *133*, 17528. (e) O'Neil, E. J.; Smith, B. D. *Coord. Chem. Rev.* **2006**, *250*, 3068. (f) Sun, H.; Hunter, C. A.; Navarro, C.; Turega, S. M. *J. Am. Chem. Soc.* **2013**, *135*, 13129.

(18) Cisse, L.; Djande, A.; Capo-Chichi, M.; Delatre, F.; Saba, A.; Tine, A.; Aaron, J.-J. *Spectrochim. Acta, Part A* **2011**, *79*, 428.

(19) Snyder, P. W.; Mecinović, J.; Moustakas, D. T.; Thomas, S. W.; Harder, M.; Mack, E. T.; Lockett, M. R.; Héroux, A.; Sherman, W.; Whitesides, G. M. *Proc. Natl. Acad. Sci. U.S.A.* **2011**, *108*, 17889.



- (20) (a) Spolar, R. S.; Livingstone, J. R.; Record, M. T. *Biochemistry* **1992**, *31*, 3947. (b) Livingstone, J. R.; Spolar, R. S.; Record, M. T. *Biochemistry* **1991**, *30*, 4237. (c) Spolar, R. S.; Ha, J.-H.; Record, M. T. *Proc. Natl. Acad. Sci. U.S.A.* **1989**, *86*, 8382. (d) Ha, J.-H.; Spolar, R. S.; Record, M. T. *J. Mol. Biol.* **1989**, *209*, 801. (e) Spolar, R. S.; Record, M. T. *Science* **1994**, *263*, 777. (f) Reynolds, J. A.; Gilbert, D. A.; Tanford, C. *Proc. Natl. Acad. Sci. U.S.A.* **1974**, *71*, 2925. (g) Serrano, L.; Sancho, J.; Hirshberg, M.; Fersht, A. R. *J. Mol. Biol.* **1992**, *227*, 544. (h) Vallone, B.; Miele, A. E.; Vecchini, P.; Chiancone, E.; Brunori, M. *Proc. Natl. Acad. Sci. U.S.A.* **1998**, *95*, 6103. (i) Takano, K.; Yamagata, Y.; Fujii, S.; Yutani, K. *Biochemistry* **1997**, *36*, 688. (j) Serrano, L.; Kellis, J. T.; Cann, P.; Matouschek, A.; Fersht, A. R. *J. Mol. Biol.* **1992**, *224*, 783.
- (21) (a) Hunter, C. A. *Angew. Chem., Int. Ed.* **2004**, *43*, 5310. (b) Andrews, P. R.; Craik, D. J.; Martin, J. L. *J. Med. Chem.* **1984**, *27*, 1648.
- (22) (a) Jiang, W.; Ajami, D.; Rebek, J., Jr. *J. Am. Chem. Soc.* **2012**, *134*, 8070. (b) Ajami, D.; Rebek, J., Jr. *Nat. Chem.* **2009**, *1*, 87. (c) Asadi, A.; Ajami, D.; Rebek, J., Jr. *J. Am. Chem. Soc.* **2011**, *133*, 10682. (d) Rebek, J., Jr. *Chem. Commun.* **2007**, 2777.
- (23) (a) Inokuma, Y.; Yoshioka, S.; Ariyoshi, J.; Arai, T.; Hitora, Y.; Takada, K.; Matsunaga, S.; Rissanen, K.; Fujita, M. *Nature* **2013**, *495*, 461. (b) Kawano, M.; Fujita, M. *Coord. Chem. Rev.* **2007**, *251*, 2592. (c) Nassimbeni, L. R.; Su, H. *CrystEngComm* **2013**, *15*, 7396. (d) Inokuma, Y.; Arai, T.; Fujita, M. *Nat. Chem.* **2010**, *2*, 780. (e) Bradshaw, D.; Claridge, J. B.; Cussen, E. J.; Prior, T. J.; Rosseinsky, M. J. *Acc. Chem. Res.* **2005**, *38*, 273.
- (24) Metherell, A. J.; Cullen, W.; Stephenson, A.; Hunter, C. A.; Ward, M. D. *Dalton Trans.* **2014**, 43, 71.
- (25) *MacroModel*, version 9; Schrödinger, LLC: New York, 2011.
- (26) *Spartan'06*; Wavefunction, Inc.: Irvine, CA, 2006.
- (27) Coles, S. J.; Gale, P. A. *Chem. Sci.* **2012**, *3*, 683.
- (28) Sheldrick, G. M. *Acta Crystallogr., Sect. A* **2008**, *64*, 112.
- (29) Dolomanov, O. V.; Bourhis, L. J.; Gildea, R. J.; Howard, J. A. K.; Puschmann, H. *J. Appl. Crystallogr.* **2009**, *42*, 339.